P. A. Terpstra,
C. Otto,
J. Greve
University of Twente
Department of
Applied Physics
Applied Optics Group
P.O. Box 217
7500 AE Enschede
The Netherlands

Received 3 June 1996;
accepted 9 October 1996

Subpicosecond Dynamics in Nucleotides Measured by Spontaneous Raman Spectroscopy

Abstract: *The band widths in Raman spectra are sensitive to dynamics active on a time scale from 0.1 to 10 ps. The band widths of nucleotide vibrations and their dependence on temperature, concentration, and structure are reported. From the experimental band widths and second moments, it is derived that the adenine vibrations at 725, 1336, 1480, and 1575 cm^{-1}, and the uracil vibration at 787 cm^{-1}, are in the fast modulation limit. The correlation times of the perturbations are faster than 0.4 ps. Thermal melting of the helical structure in polynucleotides results in larger band widths, due to an increase in vibrational dephasing and energy relaxation as a consequence of the increased interaction of the base moieties with the solvent molecules. The band width of the 725 cm^{-1} adenine vibration is dependent on the type and structure of the backbone. It is found to be perturbed by movements of the sugar–phosphate moiety relative to the base. The band width of the 1575 cm^{-1} adenine vibration is found to be sensitive to the base-pairing interaction.*

From a comparison of the band widths in polynucleotides with a different base sequence (homopolymer vs alternating purine–pyrimidine sequence), it is concluded that resonant vibrational energy transfer between the base molecules is not important as a relaxation process for the vibrational band widths of nucleotides. Several theoretical models for the interpretation of band widths are discussed. The theory does not take into account the strong hydrogen-bonding nature water and hence fails to describe the observations in nucleotide–water systems. The bands of the carbonyl stretching vibrations are inhomogeneously broadened. The carbonyl groups have a strong dipolar interaction with the polar water molecules and are therefore strongly perturbed by coupling to the heatbath via hydrogen bonds. © *1997 John Wiley & Sons, Inc. Biopoly* ***41:*** *751–763, 1997*

Keywords: *Subpicosecond dynamics; nucleotides; spontaneous Raman spectroscopy*

INTRODUCTION

Raman spectra of complex molecules do not consist of a set of sharp lines, as time-dependent forces broaden the vibrational bands. Raman band widths in polynucleotides range from 8 wavenumbers to 35 wavenumbers, and the corresponding time scale of the perturbing forces ranges from fractions of a picosecond to several picoseconds. Vibrational frequencies depend on static molecular parameters as

Correspondence to: C. Otto
Contract grant sponsor: Netherlands Organization for the Advancement of Research

CCC 0006-3525/97/070751-13

force constants, bond distances and angles, atomic masses, and electric charges. Dynamic parameters of atomic and molecular motions determine the vibrational band shapes. A number of processes have been distinguished that broaden the vibrational bands in the frequency domain. The theory is well covered in a few papers[1–8] and a recent overview also covers a comparison between experimental results and theoretical predictions.[9]

Most investigations on Raman band width effects have been done for simple molecules in low viscosity environments, where vibrational dephasing dominates the band width.[1,2,10,11,12] In this paper, the more complex system of polynucleotides in an aqueous buffer solution is studied. Polynucleotides are complex polymers arranged in single- or double-stranded helical structures. In a double-stranded helix, the bases are on the inside of the helix and are hydrogen bonded to the bases of the complementary strand. The first hydration shell[13] consists of 20 molecules of water per nucleotide in native B-DNA. Of these molecules, 11–12 are in direct contact with DNA and are tightly bound. This inner primary hydration shell is impermeable to cations and does not freeze into an ice-like state at temperatures well below 0°C. A secondary hydration shell of loosely bound water molecules surrounds this structure. Many dynamical processes, such as vibrational energy exchange, vibrational resonance coupling, vibrational dephasing, and rotational broadening[14,15] may occur in this system in the (sub)picosecond time domain, which may contribute to the band width of the vibrational modes. A number of dynamical processes in a nucleotide–water system occur sufficiently frequent to contribute to dephasing: (1) Translational and rotational times of water molecules and rearranging times of water–water clusters are on the order of 1–10 ps, according to Finney et al.[16] Ohmine et al.[17] report for the molecular dynamics of water that on average the hydrogen bonds of every water molecule are broken every 10 ps and that cluster rearranging times are in the order of 30 ps. (2) For dynamics in the sugar group, sugar repuckering in nucleotides takes place every 0.5–1.8 ps.[18] Some base vibrations have part of their potential energy distributed over the backbone,[19] and they may then also be modulated by these perturbations. (3) For dynamics in the backbone, motions of molecular groups occur on a (sub)picosecond time scale. The measured time for a rotation of 180° of a buried tyrosine in protein takes 0.5–1 ps[20] and the rotational tumbling motion of free benzene through an angle of 41° takes 2.6–2.8 ps.[14,15] Base vibrations that are coupled to backbone vibrations may be modulated by these type of movements. (4) For hydrogen bond breaking and formation, hydrogen bond breaking times are on the order of 0.5 ps[21] to 2–3 ps.[17] Indirect dephasing may occur via hydrogen bonds between nucleotide and the solvent, acting as the heat bath.

Since polynucleotides have a nicely defined structure, it can be anticipated that different vibrations will have a different coupling to the existing degrees of freedom. It may thus be possible to distinguish between the different types of perturbations. Another way is to compare changes of the band width with predictions by theoretical models. The rate of vibrational dephasing, for example, depends on the number of collisions, which in turn is dependent on the temperature, density, and the viscosity of the solution. Resonant vibrational energy exchange is dependent on the orientation of and distance between the interacting molecules. So polynucleotides with different structure and base compositions will have different rates of vibrational resonance exchange. In this paper, Raman band widths of nucleotide spectra will be compared with theoretical models. Also, the dependence of different vibrations on nucleotide structure and base composition will be reported.

MATERIALS AND METHODS

Chemicals

From Sigma we purchased the mononucleotides 5′-rAMP (lot no. 90H7215), 5′-dAMP (lot no. 66C-7040), 5′-rATP (lot no. 29F7110), and 5′-rUMP (lot no. 48F05481). The 3′-dTMP was obtained from PL-biochem. (lot no. 654162) and adenine was obtained from Serva (lot no. 10739). The polynucleotides were purchased from Pharmacia, poly(rA) (lot no. AA4110P01), poly(dA) (lot no. 3017836011), poly(rU) (lot no. AB4440P08), poly(rA)·poly(rU) (lot no. QH8245-2101), poly(rA-rU)·poly(rA-rU) (lot no. AA7990P03), poly(dA)·poly(dT) (lot no. 2107860011) and poly(dA-dT)·poly(dA-dT) (lot no. AE7870108). All the nucleotides were used without further purification and were dissolved in an aqueous buffer solution containing 93 m*M* NaCl, 10 m*M* Na_2HPO_4, 7 mM NaCacodylate and the pH of the buffer was 7.2. The concentrations were 78 m*M* for 5′-rAMP and 5′-rATP, 20 m*M* for 5′-dAMP, 7 m*M* for adenine, and 40 m*M* for 3′-dTMP. The concentrations for the single-stranded polynucleotides were 78 m*M* bases for poly(rA) and 14 m*M* bases for poly(dA). The double-stranded polynucleotides were dissolved in the concentrations of 14 m*M* base pairs for poly(rA)·poly(rU) and 10 m*M* base pairs for poly(rA-rU)

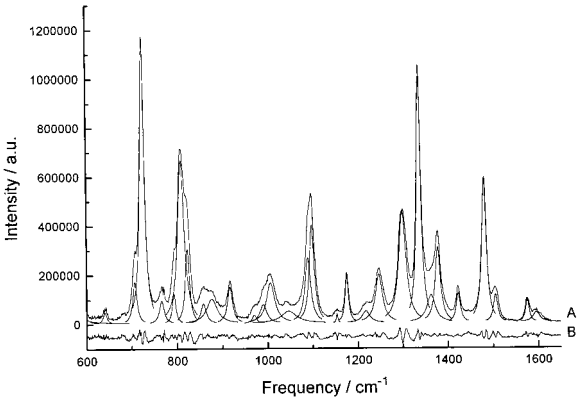

FIGURE 1 The isotropic Raman spectrum of poly(rA) at 14°C with the curvefit results. (A) Raman spectrum; (B) residue spectrum = Raman spectrum − Fit results.

·poly(rA-rU), poly(dA)·poly(dT), and poly(dA-dT)·poly(dA-dT).

Equipment

The experimental equipment has been described previously.[22] The spectra for 5′-rAMP, 5′-rUMP, 3′-dTMP, poly(rA), and poly(rU) were recorded with 15 s per spectral point. The spectra of adenine, poly(dA), and the double-stranded polynucleotides were recorded with 55 s per spectral point. The spectra are deconvolved for the instrument response. The instrument profile was determined by measuring the response of the setup to the emission of an Argon laser at 514.5 nm and the emission of a Helium-Neon laser at 632.8 nm. The best approximation for the instrument profile is a Gauss curve with a band width of 3 cm^{-1}. The band widths of the lasers were ≤ 0.2 cm^{-1}. The spectra have been curve fitted with the RAMPAC program.[23]

RESULTS

The development of fast and accurate curve fitting programs allows the analysis of the vibrational spectra of complicated biological molecules containing often more than 40 vibrational bands.[22,23] The quantitative information concerns the following: (1) the position, indicative of the force field; (2) the integrated intensity, which is sensitive to local structure and stacking interactions; and (3) the band width, which gives information about the (sub)picosecond dynamics. Figure 1 gives a typical example of the quality of the curve fitting of nucleotide spectra. In this paper we will concentrate on the vibrational band widths.

We measured for all the samples the ∥ (vertically polarized excitation and vertically polarized scattered light) and ⊥ (horizontally polarized excitation and vertically polarized scattered light) spectra. From these spectra the isotropic and anisotropic spectrum can be calculated[24]:

$$I_{iso} = I_{\parallel} - \tfrac{4}{3} I_{\perp} \quad (1)$$

$$I_{aniso} = I_{\perp} \quad (2)$$

Only the strongest base vibrations are studied in this paper. For uracil, these are the 787 cm^{-1} ring vibration and the carbonyl vibrations at 1690 cm^{-1}. For thymine, we studied the 743, 781, and 1373 cm^{-1} ring vibrations, and the carbonyl vibrations at 1660 cm^{-1}. For adenine, the strongest vibrations are the 725, 1336, 1480, and 1575 cm^{-1} base vibrations. The 725 and 1480 cm^{-1} adenine vibrations are located in the pyrimidine and the imidazole ring. The 1336 and the 1575 cm^{-1} adenine vibrations are predominantly located in the pyrimidine ring.[25,26]

The band widths of the base vibrations have been measured as a function of the temperature for adenine, 5′-rAMP, 5′-rUMP, poly(rA), and poly(rU) (Tables I–III). Only the results for the extreme temperatures are given. But the band widths have been measured at 4 different temperatures for the mononucleotides, and at 8 different temperatures for the polynucleotides. The concentration dependence

Table I Bandwidths (cm^{-1}) of Adenine Vibrations in Mononucleotides*

Nucleotide	725 cm^{-1}	1336 cm^{-1} Isotropic	1336 cm^{-1} Anisotropic	1480 cm^{-1}	1575 cm^{-1}
5′-rAMP 75°C	15.5 ± 0.5	16.6 ± 0.5	17.3 ± 0.5	16.0 ± 1	13.1 ± 0.8
5′-rAMP 5°C	16.5 ± 0.5	16.0 ± 0.5	16.8 ± 0.5	15.0 ± 1	13.0 ± 0.8
5′-rATP	15.1 ± 0.5	15.8 ± 0.5	16.8 ± 0.5	14.8 ± 1	12.2 ± 0.8
5′-dAMP	11.3 ± 0.5	15.9 ± 0.5	17.3 ± 0.5	14.9 ± 1	12.4 ± 0.8
Free adenine	8.6 ± 0.5	13.7 ± 1			

* The errors in this table and all following tables are based upon the error calculation described in Refs. 23 and 45.

Table II Bandwidths (cm^{-1}) of the Uracil 787 cm^{-1} Uracil Vibration

Nucleotide	Bandwidth
5′-rUMP 75°C	12.7 ± 0.5
5′-rUMP −10°C	12.2 ± 0.5
Poly(rU) 45°C	11.0 ± 0.5
Poly(rU) −6°C	7.5 ± 0.5
Poly(rA)·poly(rU)	8.3 ± 1
Poly(rA-rU)·poly(rA-rU)	8.5 ± 1

has been measured for 5′-rAMP and 5′-rATP (Figure 2). The Raman band widths of base vibrations have also been measured for 3′-dTMP (Table IV) and the stacked polynucleotides poly(rA)·poly(rU), poly(rA-rU)·poly(rA-rU), poly(dA)·poly(dT), and poly(dA-dT)·poly(dA-dT) (Tables II–IV). The vibrational frequencies for the strong base vibrations change between the different nucleotides as a result of changes in the force constants. We use the frequencies of the adenine normal modes in poly(rA), the uracil normal modes in poly(rU), and the thymine modes in 3′-dTMP to identify the normal modes. Most of the base vibrations are stronger in the isotropic spectrum and these band widths are presented in the tables. The 1575 cm^{-1} adenine base vibration is, however, stronger in the anisotropic spectrum, and for this band the anisotropic band widths are shown. In the absence of reorientational broadening, as is the case for polynucleotides (see below), this does not make a difference.

Due to overlap with adenine base and phosphate vibrations, we were not able to measure the band widths for the 781 and 1373 cm^{-1} thymine vibrations in double-stranded deoxyribonucleotides. In polydeoxyribonucleotides, the 1336 cm^{-1} adenine vibration splits in two components at 1332 and 1344 cm^{-1}.[27] This prohibited the measurement of the band widths of these vibrations in this case.

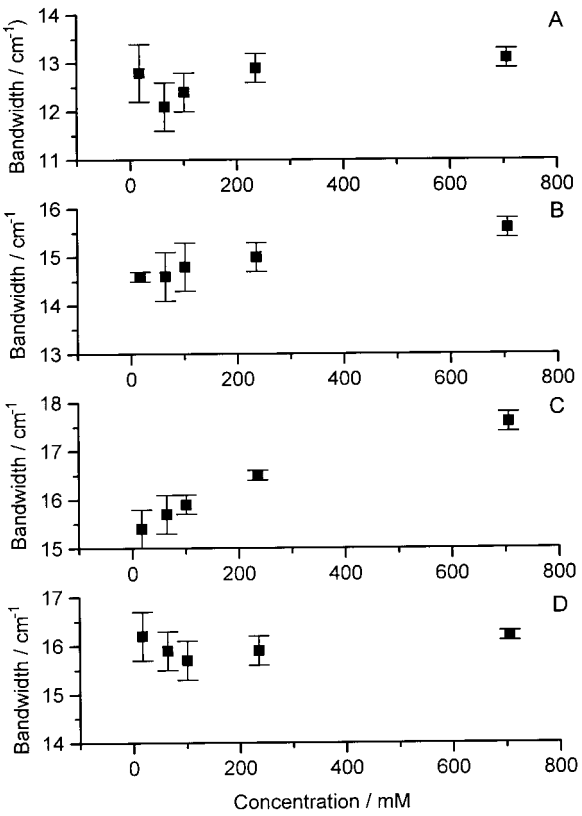

FIGURE 2 Bandwidths of adenine base vibrations in 5′-rAMP as a function of the concentration. (A) The 1575 cm^{-1} adenine vibration; (B) 1480 cm^{-1} adenine vibration; (C) 1336 cm^{-1} adenine vibration; (D) 725 cm^{-1} adenine vibration.

Apart from the band width data above, we observed a frequency change of the 787 cm^{-1} uracil vibration upon melting of poly(rU). In stacked and unstacked poly(rU), the frequencies are respectively 787 and 783 cm^{-1}. During the melting transi-

Table III Bandwidths (cm^{-1}) of Adenine Vibrations in Polynucleotides

Polynucleotide	725 cm^{-1}	1336 cm^{-1}	1344 cm^{-1}	1480 cm^{-1}	1575 cm^{-1}
Poly(rA) 75°C	12.8 ± 0.5	16.4 ± 0.5		16.0 ± 1	13.8 ± 0.8
Poly(rA) 5°C	11.5 ± 0.5	11.1 ± 0.5		13.0 ± 1	11.7 ± 0.8
Poly(dA) 75°C	10.2 ± 0.5				
Poly(dA) 5°C	9.3 ± 0.5		14.2 ± 1	13.0 ± 1	11.4 ± 0.8
Poly(rA)·poly(rU)	11.6 ± 0.5	13.1 ± 1		13.5 ± 1	8.9 ± 0.8
Poly(rA-rU)·poly(rA-rU)	11.7 ± 0.5	13.0 ± 1		13.1 ± 1	8.9 ± 0.8
Poly(dA)·poly(dT)	7.8 ± 0.5			13.2 ± 1	9.5 ± 0.8
Poly(dA-dT)·poly(dA-dT)	8.5 ± 0.5			14.4 ± 1	9.7 ± 0.8

Table IV Bandwidths (cm^{-1}) for Thymine Vibrations

Nucleotide	743 cm^{-1}	781 cm^{-1}	1373 cm^{-1}
3′-dTMP	22.0 ± 0.7	16.9 ± 0.7	15.5 ± 0.7
Poly(dA)·poly(dT)	10.3 ± 0.5		
Poly(dA-dT)·poly(dA-dT)	11.6 ± 0.5		

tion, both vibrational bands are visible in the Raman spectrum and change in relative intensity upon melting. In 5′-rUMP, the frequency is 783 cm^{-1}.

DISCUSSION

First, the measured band width differences between the isotropic and anisotropic spectra for mononucleotides will be discussed.

Reorientational Broadening

The approach of Bartoli and Litovitz[15] was followed to obtain reorientation times from the band width differences in the anisotrpic and isotropic spectra for 5′-rAMP, 5′-dAMP, and 5′-rATP. The measurements showed a band width difference between the anisotropic and the isotropic spectrum of the 1336 cm^{-1} adenine base vibration of 0.8 ± 0.5 cm^{-1} for 5′-rAMP in H_2O and D_2O. For 5′-dAMP we observed for this band a band width difference of 1.4 ± 0.5 cm^{-1} and for 5′-rATP a band width difference of 1 ± 0.5 cm^{-1}. From this, correlation times τ_2 of reorientational motion of 13 ps for 5′-rAMP, 11 ps for 5′-rATP and 7.5 ps for 5′-dAMP can be calculated. Where τ_2 refers to the time it takes the molecule to rotate through 41°.[28,29] For other base vibrations, this calculation has not been performed, as only the 1336 cm^{-1} vibration is strong in both the isotropic and the anisotropic spectra. The 1575 cm^{-1} vibration may be used in D_2O, but the isotropic spectrum in H_2O is perturbed by residues from the H_2O bending vibration, which is much stronger than the base vibrations.

If 5′-rAMP is considered folded as a sphere with a radius of 3 Å, then τ_{De} = 26.5 ps can be derived from the Debye model for a small step diffusional rotation. The reorientational time for a free rotor is then τ_{Fr} = 1.8 ps.[29,30] The measured rotation times are in between these extremes.

For the poly(rA), the isotropic and anisotropic band widths of the 1336 cm^{-1} adenine vibration are equal. The absence of reorientational broadening in polynucleotides indicates that the bases in the polynucleotides reorient through an angle of 41° in times slower than 21 ps. A band width difference between the anisotropic and isotropic band widths of 0.5 cm^{-1}, the error margin, yields a τ_2 of 21 ps.

Fast or Slow Perturbations?

The influence of the time dependence of the perturbing forces on the time dependence of the vibrational correlation function has been derived in literature.[3,22] If the time dependence of the perturbing forces is fast compared to the vibrational correlation time, the bandshape will be Lorentzian with a band width $\Delta\nu$ (Hz) of

$$\Delta\nu = 2\tau_c\langle\,|\omega_1(0)|^2\rangle = 2\pi c\Delta\tilde{\nu} \qquad (3)$$

where τ_c is the correlation time of the perturbing forces, and ω_1 is the frequency shift due to the perturbations and $\Delta\tilde{\nu}$ is the band width in cm^{-1}.

The fitting procedure and fast Fourier transform (FFT) revealed that the band shapes of the strong base vibrations are at least 90% Lorentzian, with the carbonyl vibrations as the only exceptions (Figures 1 and 3). For a Lorentz band shape, the relation

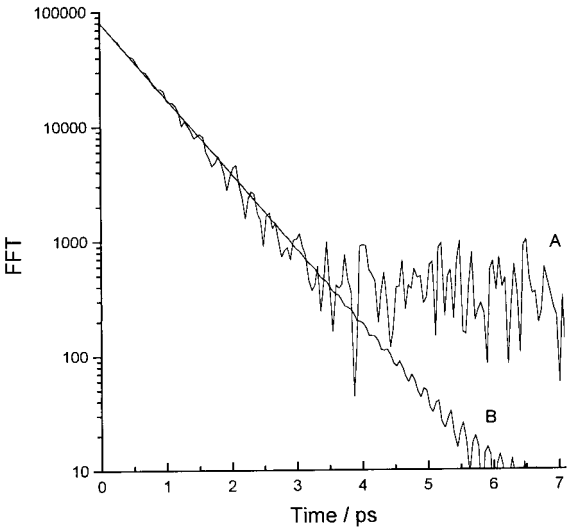

FIGURE 3 FFT of the 731 cm^{-1} adenine vibration of 5′-rAMP (A), with the FFT of a Lorentz curve from the curve fit (B). The results are similar.

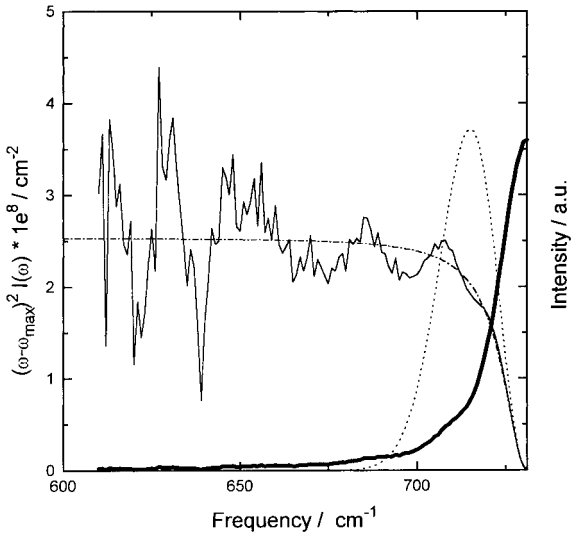

FIGURE 4 The spectrum around the 731 cm^{-1} adenine vibration in 5′-rAMP is shown (——). The neighboring bands have been subtracted with the corresponding curvefit results. The experimental second moment for this vibration is given by the area below the —— curve.

This experimental second moment is compared with the second moment for the best fit of a Lorentz band (– · – · –) and a Gauss band (· · · · ·). The best fit parameters for the Lorentz band are: ω_{max} = 730.86 cm^{-1}, FWHM = 16.4 cm^{-1}, intensity = 9.7e7; for the Gauss band: ω_{max} = 730.81 cm^{-1}, FWHM = 22.5 cm^{-1}, intensity = 1.1e8.

between the vibrational correlation time τ_a and the band width is[3]:

$$\tau_a = 1/\pi c \Delta\tilde{\nu} \qquad (4)$$

where c is the velocity of light. As the band widths of the base vibrations are on the order of 12 cm^{-1}, the corresponding vibrational correlation times are on the order of 0.88 ps. And since the band shapes are Lorentzian, this indicates that the dynamics of the perturbations are faster than 0.88 ps.[3,4]

Rothschild[3] showed that the second moment $M(2)$ of a band profile $F(\omega)$ is equal to the time independent term $\langle|\omega_1(0)|^2\rangle$ in Eq. (3). For a Lorentzian band profile, τ_c can then be calculated with Eq. (3). But it is difficult to determine the second moment $M(2)$ in complex spectra (Figure 4).[10,22,31] In order to eliminate overlapping bands, fitted Lorentz curves were subtracted and the calculation was limited to 6 times the vibrational band width.[22] However, for a Lorentzian band profile, it can be shown that because of this constraint the calculation always yields $\tau_a/\tau_c \sim 3.5$. So comparison of $M(2)$, τ_a and τ_c for different nucleotides does not give additional information, as there is a direct relation with the band width data. The results for the base vibrations show that the modulation regime is in the rapid regime for all the Lorentz band profiles (Table V). The modulation regime may extend to the very rapid modulation regime, due to the lower estimates of $M(2)$ used in these calculations. The carbonyl vibrations of uracil and thymine do not have Lorentz band shapes and are discussed below.

We conclude that all the strong base vibrations (except the carbonyl vibrations) are in the fast modulation regime. In the next sections the classification of the perturbations that modulate the vibrational motions is discussed.

Consequences of the Application of the Theoretical Models for Solvents to Aqueous Solutions

Available models[5,6,7,8] present expressions that relate the Raman band widths with temperature, viscosity, density, and oscillator frequency. If the density and viscosity of water are introduced into the equations for the vibrational band widths, it shows a decrease of approximately 80% with a temperature increase from 0 to 100°C. But from Tables I and II it can be seen that the band widths of the mononucleotides in water are insensitive to temperature changes from −10 to 75°C.

That the theoretical models are not able to describe the experimental band widths for nucleotides in an aqueous solution is partly due to the inherent restrictions of the models used. The models for vibrational dephasing, which use the hydrodynamic theory, work best for low viscosity liquids.[5–7] But in viscous liquids, the hydrodynamic theory breaks down at high frequencies.[6] This is illustrated by the hydrodynamic collision time in water $\tau_H = \rho d^2/6\eta$ = 0.0021 ps, which does not compare well with the measured perturbation time τ_c = 0.18 ps calculated from the band profile in 5′-rAMP. Navarro et al.[32] observed for the C═O vibration of trichoroacetate in different solvents that the perturbation time τ_c is also larger than the hydrodynamic collision time.

Also, the models for vibrational dephasing take only into account the repulsive part of the intermolecular potential and do not treat any interactions like hydrogen bonding. In the binary collision model,[5] for example, effects like viscosity are introduced into the model through an estimation of the time between collisions $\tau_c = \tau_H = \rho d^2/6\eta$—it does not enter into the model itself. Our solvent is, however, water, which has strong intermolecular di-

Table V The Determination of the Modulation Regime for the 725 cm^{-1} Adenine Vibration for Different Structures

	FWHM (cm^{-1})	τ_a (ps)	M(2) (cm^{-2})	τ_c (ps)
5′-rAMP 5°C	16.6	0.64	234	0.19
Poly(rA) 5°C	11.8	0.90	118	0.27
Poly(dA) 14°C	9.5	1.12	93	0.27
Poly(dA-dT)·poly(dA-dT) 14°C	8.2	1.29	62	0.35

pole–dipole forces and hydrogen bonds with itself and the nucleotide. These effects are ignored by the models. The model by Lynden–Bell[8] ignores collisional dynamics, as the repulsive part of the coupling potential is ignored. Also this simplification is too drastic, as collisions by water molecules will play an important part in the vibrational dynamics.

The large decrease predicted by the models for vibrational dephasing is for a large part due to the large decrease in viscosity of water with an increase in temperature. But dissolving adenine in water breaks up the local hydrogen-bonding structure and decreases the local viscosity of the solvent. Vibrational dephasing is caused by collisions with the solvent molecules and thus the first hydration shell will mainly determine this process (see below). So the local viscosity changes will be smaller than the bulk viscosity changes, which may partly explain the insensitivity to the temperature of the band widths of the mononucleotides.

The models for vibrational energy relaxation take only into account the relaxation of vibrational energy to phonons of the heatbath. Vibrational energy relaxation of high frequency vibrational modes is then a slow process, because the phonon density of states vanishes below the Debye frequency (typically 50–100 cm^{-1}). As a result, the probability for vibrational energy relaxation is low due to the large amount of phonons needed. It has subsequently been ignored in studies of vibrational dynamics. Experiments on the CH vibration of CH_3CCl_3 and CH_3CH_2OH and on N_2 showed that vibrational relaxation is 4–10[10] times slower than vibrational dephasing, which is in agreement with calculations by Oxtoby and Rice,[1] Fisher and Laubereau,[5] and Diestler.[4] The spectra of nucleotides, however, consist of many overlapping sugar–phosphate and base vibrations. Also, water has a significant Raman intensity over the whole frequency range. The theoretical models do not describe such a situation. So vibrational energy relaxation may be fast enough to cause vibrational broadening. With coherent and incoherent time-resolved measurements, these two contributions can be separated. But it has already been shown above that the vibrational dynamics are in the subpicosecond time domain, which makes such an experiment very complicated.

As the theoretical models are not able to describe the vibrational dynamics of nucleotides, an experimental approach is used to obtain information. Different vibrations may be sensitive to different relaxation mechanisms, and this kind of information is available from our spontaneous Raman measurements.

Vibrational Dephasing and Energy Relaxation of Nucleotide Vibrations by Water Molecules

Molecular dynamics calculations of the solvation of ions in polar solvents have shown a solvation dynamics that has a two-part character. One part consists of a fast initial relaxation due to small amplitude inertial dynamics of the solvent molecules within the confines of their instantaneous environment on time scales of 0.1–0.2 ps for acetonitrile[33] and 0.025 ps for water.[34] The second much slower part, ~1 ps time scale, reflects larger amplitude motions involving the breakup and reorganization of these local environments, especially in the first hydration shell of the solvent. Rosenthal et al.[35] have confirmed these findings for acetonitrile with femtosecond fluorescence spectroscopy. Translational and rotational times of water molecules and rearranging times of water–water clusters are on the order of 1–10 ps, according to Finney et al.[16] Ohmine et al.[17] reports for the molecular dynamics of water, that on average the hydrogen bonds of every water molecule are broken every 10 ps and that cluster rearranging times are in the order of 30 ps. Comparison with the perturbation time of 0.18 ps in 5′-rAMP indicates that the perturbation by collisions with water molecules is not due to translational or

rotational motions. A rattling of water molecules in a cage determined by surrounding water molecules and the nucleotide will occur at faster time scales[17,33,34,35] and is most likely the collisional mechanism that determines the dephasing of nucleotide vibrations. An increase in exposure to water molecules will increase the dephasing rate and increase the nucleotide band widths. Also, vibrational energy relaxation to the solvent will be more effective with an increase in exposure to the solvent.

All the studied adenine, thymine, and uracil vibrations have a smaller band width in stacked structures than in unstacked structures and mononucleotides. Moreover, the band widths of the 1336, 1480, and 1575 cm^{-1} adenine vibrations increase toward the value for the mononucleotides upon melting of poly(rA). In a previous paper,[22] we have assigned this temperature behavior of the band widths of poly(rA) to an increasing exposure of the bases to the solvent upon melting of the secondary structure. In unstacked single-stranded structures, the 1336, 1480, and 1575 cm^{-1} adenine vibrations are equally perturbed by interactions with water molecules as in mononucleotides. This increasing exposure to the solvent upon melting is supported by assignments of these vibrations to base vibrations that have their potential energy distributed predominantly over the pyrimidine ring.[25,26] The pyrimidine ring will be most sensitive to an increase in exposure to the solvent upon melting of the single-stranded poly(rA), as it is located on the outside of the structure.

The base vibrations of free adenine have a smaller band width than those of 5′-rAMP, 5′-rATP, and 5′-dAMP. This may be due to the apolar character of free adenine, which will result in less interaction with surrounding water.

The band width of the 787 cm^{-1} uracil vibration of poly(rU) increases upon melting from 7.5 to 11.0 cm^{-1}, which remains 1.3 cm^{-1} below the band width of 5′-rUMP. The band width of the 725 cm^{-1} adenine vibration increases 1 cm^{-1} upon melting of poly(rA) and poly(dA), but remains also smaller than the values for the mononucleotides. This indicates that some shielding from water remains in unstacked poly(rA) and poly(rU), but perturbations by the backbone may also be the cause, as will be discussed below.

For all the vibrations studied, it is found that the more exposed a vibration is to the solvent, the larger the band width is due to interactions with the solvent. And based on the time scales discussed above, the collisions of the solvent molecules may be seen as the rattling of the solvent molecule in a cage formed by the surrounding solvent molecules and the base.

Resonant Energy Transfer

Resonant energy transfer is the transfer of the vibrational energy to the same vibrational mode on another molecule of the same species through an intermolecular coupling potential. As a result of the exact energy match, the probability for this process is large enough to be an important relaxation process. This process will be more effective if the interacting molecules are close and may in that case influence the vibrational band widths.[8,36] The mononucleotides 5′-rAMP and 5′-rATP have been measured as a function of concentration from 17 to 706 mM, and all the vibrations studied remained constant in band width as a function of concentration (Figure 2). So the vibrational dynamics of the adenine modes are insensitive to average base–base distance changes from approximately 16 Å at 706 mM to 60 Å at 17 mM. This shows that resonant energy transfer does not play a significant role for the mononucleotides in an aqueous solution. In the polynucleotides studied, the average base–base distances are on the order of 3–4 Å.[37] The base–base distances are thus significantly smaller compared to mononucleotides and resonant energy transfer is expected to be very effective at these distances, if there is an intermolecular coupling potential. The vibrational band widths of the polynucleotides are, however, smaller than in mononucleotides. This is another indication that resonant energy transfer is not an important relaxation mechanism. Likewise, no band width differences can be observed between homo- and copolymers for the adenine vibrations at 725, 1336, 1480, and 1575 cm^{-1}, and the 787 cm^{-1} uracil vibration. So changes in base–base overlap and orientation do not influence the band width. This shows that, also in polymers, resonant energy transfer is not a relaxation path and that there is no significant intermolecular coupling potential that couples the vibrational motions on different bases of the same species.

Vibrational Dephasing of Nucleotide Vibrations by the Sugar Phosphate Backbone

Vibrational dephasing of the sugar vibrations may occur due to sugar repuckering or due to movements of the base relative to the sugar–phosphate moiety, as has been discussed in the introduction. Base vibrations that are coupled to the backbone vibrations

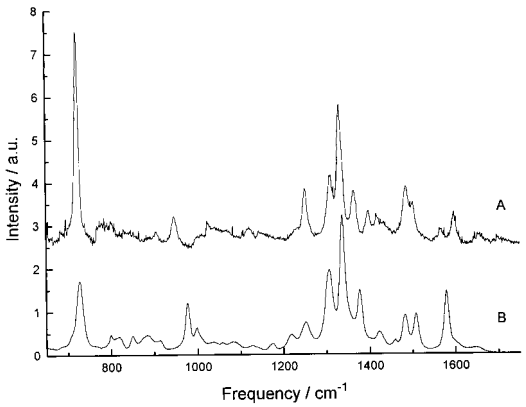

FIGURE 5 The total Raman spectra ($\| + \perp$) of adenine at 14°C (A) and 5′-rAMP at 5°C (B). Both spectra are normalized for laser intensity, measuring time, and concentration. The intensity of the 725 cm^{-1} adenine vibration compared to the intensity of the other base vibrations is much larger in adenine than in 5′-rAMP.

or that have part of their potential energy distributed over the backbone may also be modulated by these mechanisms. The 725 cm^{-1} adenine vibration is very sensitive to the type and structure of the backbone, so it appears to be modulated by these interactions.

This vibration is assigned to the breathing mode of the benzene ring of the adenine molecule. Normal mode calculations by Letellier et al.[19] and Majoube[38] showed modes with frequencies around 725 cm^{-1} that are strongly coupled to the glycosidic bond. This vibration is most sensitive to $C_{1'}-D$ substitution, which also shows the coupling of this vibration to the backbone.[25] Moreover, the intensity of this vibration is sensitive to the type of backbone. The intensity of the 725 cm^{-1} vibration relative to all other vibrations is much larger in free adenine, where there is no ribose group at all attached to the base, compared to 5′-rAMP (Figure 5). Both are mononucleotides, so the hypochromic effect cannot account for this difference. It has to be linked directly to the backbone. Majoube[38] suspected that the 725 cm^{-1} mode of adenine loses a large part of its energy as a result of a coupling to the sugar–phosphate moiety in 5′-rAMP.

The band width of the 725 cm^{-1} vibration in free adenine is smaller than the band width in stacked poly(rA). It is improbable that adenine dissolved in an aqueous buffer is stacked, as no changes in the spectra have been observed between 14 and 75°C. Thus shielding from the solvent cannot explain the behavior of the band width of the 725 cm^{-1} vibration. Further measurements on polynucleotides revealed that the band width of the 725 cm^{-1} vibration is sensitive to the type of backbone and the single or double strandedness of the polynucleotide (Table III).

Comparing the data for ribonucleotides and for the deoxyribonucleotides separately, it is observed that the band width of the 725 cm^{-1} adenine vibration is much larger in the mononucleotides than in the polynucleotides. Even melting the single-stranded helix does not eradicate this large band width difference. The band width difference for the 725 cm^{-1} adenine vibration remains very large between unstacked poly(rA) and poly(dA) compared to, respectively, 5′-rAMP and 5′-dAMP. But no differences can be observed between stacked single-stranded and double-stranded structures. We propose that the larger mobility of the sugar phosphate moiety in mononucleotides causes this increase in band width. The fluctuations of the sugar group relative to the base around the glycosidic bond distorts the bonds that take part in the 725 cm^{-1} adenine vibration. This will perturb the phase of the vibration by introducing many small frequency shifts. Such a perturbation will show up as vibrational dephasing in Raman spectra. In free adenine, the sugar group is absent and should not perturb the vibration. This is reflected by the band width, which is for adenine smaller than for 5′-rAMP and 5′-dAMP. The larger mobility of sugar–phosphate moiety in mononucleotides may also cause the 1 cm^{-1} band width difference between unstacked poly(rU) and 5′-rUMP, instead of a remaining shielding from the solvent.

By taking the mononucleotides and the polynucleotides separately, it can be observed that the band width of the 725 cm^{-1} adenine vibration is larger in ribonucleotides than in deoxyribonucleotides. So the type of backbone has also an influence on the Raman band width. The sensitivity of optical properties of the base to the type of backbone has been observed with CD spectra of 5′-rAMP and 5′-dAMP, which differ as a result of differences in the orientation of the sugar–phosphate moiety relative to the base (glycosidic bond angle). Deoxyribonucleotides, however, are found to exist in more different helical structures and with more different sugar puckers than ribonucleotides.[37] This is in contrast with the smaller band width of the 725 cm^{-1} adenine vibration in deoxyribonucleotides, as it indicates a less perturbed or less dynamic structure. Apparently, the dynamics measured by Raman band widths are very localized and measure the rigidity of the local base–backbone bond. Comparison with melting temperatures of the different structures[39]

Table VI Comparison of the Bandwidth of the 725 cm^{-1} Adenine Vibration with Melting Temperatures for Polynucleotides (100 m*M* Na^+)

Polynucleotide	725 cm^{-1}	Melting-Temperature (°C)
Poly(rA) 75°C	12.8	45
Poly(rA) 5°C	11.5	
Poly(dA) 75°C	10.2	50
Poly(dA) 5°C	9.3	
Poly(rA)·poly(rU)	11.6	57
Poly(rA-rU)·poly(rA-rU)	11.7	63
Poly(dA)·poly(dT)	7.8	66
Poly(dA-dT)·poly(dA-dT)	8.5	60

does not give a relation with the band widths (Table VI). But this is not surprising, as the stability of the helix is determined for the larger part by the base–base interaction energy.

Indirect Dephasing of Carbonyl Vibrations Through Coupling to Hydrogen Bonds

The carbonyl vibrations of uracil and thymine have much larger band widths than other base vibrations. The carbonyl vibrations of uracil have in 5′-rUMP and poly(rU) even a Gaussian band shape, whereas the carbonyl vibration in 3′-dTMP has a Voigt band shape. A Voigt band profile is a convolution of a Lorentz curve and a Gauss curve. So the vibrational dynamics of these vibrations are very different from the other base vibrations. This is probably due to hydrogen bonding, as the carbonyl bonds of uracil and thymine are hydrogen bonded to water in single-stranded structures and mononucleotides, and to the complementary base and water in double-stranded structures.[13]

A low frequency mode, like a hydrogen-bond stretch vibration, is highly perturbed by the environment due to the low energy difference between the vibrational energy and the energy levels of the heat bath. A high frequency mode that couples to this low frequency mode, as the carbonyl vibrations, may then be perturbed by the heat bath via the low frequency mode.[40,41] Robertson and Yarwood[41] described indirect dephasing for overdamped and underdamped hydrogen bonds and the slow, intermediate and fast modulation regimes.

Water–water hydrogen bonds have stretching frequencies of 190 cm^{-1}, so the period is 0.18 ps.[42] Hydrogen-bond breaking times have been derived to be in the order of 0.5 ps[21] to 2–3 ps[17] and rotational and translational times are 1–10 ps,[16] so the hydrogen bond is able to complete full periodic cycles. Moreover, the stretching vibration of water–water and water–salt hydrogen bonds[43] can be observed in low frequency Raman spectra as a vibrational band.[42,43] This shows that these hydrogen bonds are underdamped. It is therefore most likely that the carbonyl–water hydrogen bonds are also underdamped. From the models for indirect dephasing, it can be derived that, for an underdamped hydrogen-bond vibration and the intermediate perturbation regime, combination bands will appear at the sum frequencies around the high frequency mode. But these are not observed in our spectra. Based on the Gaussian band profile of the carbonyl vibrations in poly(rU) and 5′-rUMP and the absence of combination bands, the vibrations are in the slow modulation regime. Robertson and Yarwood[41] showed that for the slow modulation limit and an underdamped low frequency mode, the coupling between the low and high frequency mode is strong.

The carbonyl vibrations in stacked poly(rU) (−3°C) show three Gaussian components at 1662, 1691, and 1714 cm^{-1} (Figure 6). Only two vibra-

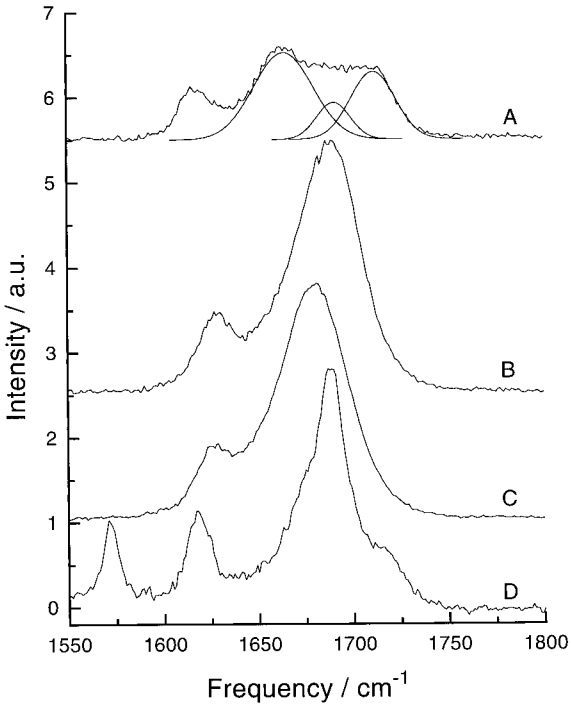

FIGURE 6 The double-bonded stretch vibrations (C═C, C═O). (A) Poly(rU) at −3°C; (B) poly(rU) at 45°C; (C) 5′rUMP at 22°C; and (D) poly(rA)·poly(rU) at 5°C.

tions are expected, the $C_4{=}O$ and $C_2{=}O$ vibrations. These vibrations are apparently highly coupled to C=C vibrations. Upon unstacking of poly(rU), one strong component at 1690 cm^{-1} dominates the spectrum in this frequency region. The shape for unstacked poly(rU) is identical to the carbonyl vibrations in 5′-rUMP, which has a strong band at 1680 cm^{-1}. The band widths for the strong components are 35 ± 5 cm^{-1}. The weaker components have similar band widths, but the error is much larger. These observations lead to a picture of a wide distribution of water–carbonyl hydrogen bonds coupled to the carbonyl stretch vibration. This leads to an inhomogeneously broadened carbonyl stretching mode. The carbonyl oscillator is coupled to the bath through a hydrogen-bonded solvent molecule. In this way, bath dynamics causes indirect dephasing in the slow modulation limit according to the models mentioned above. In the double-stranded ribonucleotides poly(rA)·poly(rU) and poly(rA-rU)·poly(rA-rU), three components also can be observed at 1668, 1688, and 1716 cm^{-1}. The band widths are smaller (17 ± 5 cm^{-1}) than in poly(rU) or 5′-rUMP and the band shape is more Lorentzian (Figure 6). This change in band shape may indicate a faster indirect dephasing mechanism, but a smaller distribution of hydrogen bonds is more likely. The more rigid double-stranded structure allows only a limited range of base–base and base–water hydrogen bonds and thus narrows the band widths.

For deoxyribonucleotides, the carbonyl vibrations behave in a similar manner. The 3′-dTMP has two vibrational bands at 1661 and 1668 cm^{-1}, which have band widths in the order of 30 cm^{-1} and Voigt band shapes. This may indicate a somewhat faster relaxation mechanism. Also the Raman spectra of double-stranded deoxyribonucleotides have narrower and more Lorentz bands for the carbonyl vibrations. Two components at 1651 and 1673 cm^{-1} with band widths of 17 ± 5 cm^{-1} are evident (Figure 7).

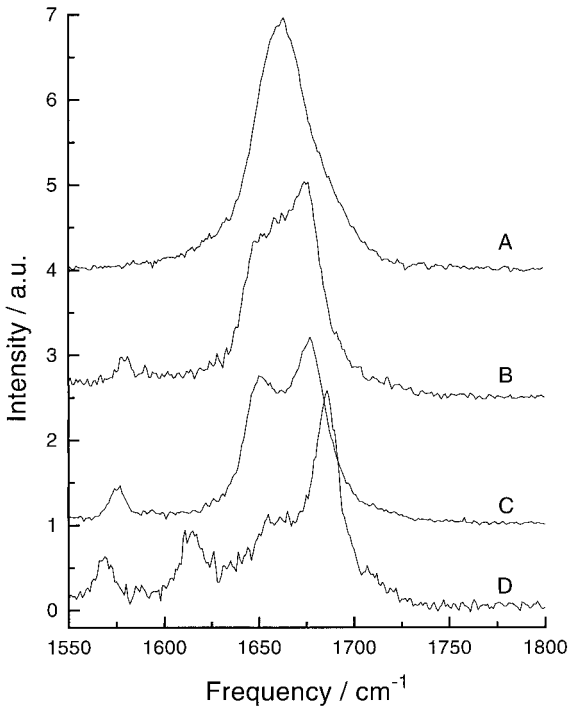

FIGURE 7 The double-bonded stretch vibrations (C=C, C=O). (A) 3′-dTMP 14°C; (B) poly(dA)·poly(dT) at 14°C; (C) poly(dA-dT)·poly(dA-dT) at 14°C; (D) poly(rA-rU)·poly(rA-rU) at 14°C.

The Effect of Hydrogen Bonding on the Bandwidth of a Ring Vibration

The 1575 cm^{-1} vibration of adenine has a similar band shape and band width compared to the other adenine ring vibrations. Also its band width increases toward the band width of 5′-rAMP upon melting of poly(rA). A large part of the vibrational dynamics has thus been attributed to vibrational dephasing and energy relaxation by water molecules. A part of the vibrational dynamics of this ring vibration is, however, sensitive to the conformation.

In mononucleotides and single-stranded polynucleotides, the adenine base is hydrogen bonded to water molecules and the band width is 11.7–13.8 cm^{-1}. In double-stranded polynucleotides, the adenine base is hydrogen bonded to the complementary base and the band widths are smaller: 8.9 to 9.7 cm^{-1}. Apparently, this vibration is sensitive to base–base or base–water hydrogen bonding. This is in accordance with the fact that this vibration is predominantly located in the pyrimidine ring.[25,26]

Water molecules are not kept at certain positions by restrictions through secondary structure, as the complementary bases are. Hence, water–base hydrogen bonds are a less stable conformation than base–base hydrogen bonds. The wider distribution of water–water hydrogen bond lengths and angles will increase the band width through indirect dephasing, as can be seen from the spectra.

CONCLUSIONS

From the band width differences between anisotropic and isotropic spectra, the rotational correlation times for mononucleotides have been derived.

The 5′-rAMP reorients through an angle of 41° in 13 ps, 5′-rATP in 11 ps, and 5′-dAMP in 7.5 ps. These times are in between the rotation times for a free oscillator and the rotation in viscous liquids. Polynucleotides reorient in times slower than 21 ps.[44]

The perturbation correlation times for the base vibrations with Lorentz band shapes were determined from experimental band width and the second moment analysis. The vibrational relaxation processes have a correlation time in the order of 0.3 ps or smaller. The vibrational correlation times are $\sim$ 1 ps and the vibrational dynamics is therefore the rapid modulation regime. The nature of the relaxation processes remains unclear. No satisfactory correlation with any of the models was obtained.

Comparison of the band widths of different vibrations in different nucleotide structures presents information about the nature of relaxation processes that perturb the base vibrations. It is found that vibrational dephasing and energy relaxation by interactions with water molecules plays an important role in the vibrational dynamics. The temperature dependence of the band widths of the 1336, the 1480, and the 1575 cm^{-1} vibrations of adenine in poly(rA) and the 787 cm^{-1} vibration of uracil in poly(rU) increase toward the value of the mononucleotides as a result of the melting of the single-stranded structures. Also, the thymine base vibration at 743 cm^{-1} has a larger band width in 3′-dTMP compared to stacked structures. It follows that for a large number of ring vibrations an increased exposure to the water environment leads to a larger band width. The smaller band widths of free adenine compared to mononucleotides are probably due to the apolar character of the free base. This will result in less interactions with the water environment and as such to a smaller band width.

Resonant vibrational energy transfer has not been observed to play an important role as a relaxation process for nucleotides. The band width changes in base vibrations do not seem to depend on the base–base distances in the polynucleotides poly(rA-rU)·poly(rA-rU) and poly(rA)·poly(rU); poly(dA-dT)·poly(dA-dT) and poly(dA)·poly(dT). Also no dependence was observed as a function of the concentration of 5′-rAMP and 5′-rATP.

The dependence of the band width of the 725 cm^{-1} adenine vibration on the type of backbone is direct evidence that the backbone influences the band width. This proposition of the sugar–phosphate moiety as an additional perturber for the 725 cm^{-1} adenine vibration is in accordance with the small band width for the free adenine base (Table I) and the normal mode description.

The band widths of the carbonyl vibrations of uracil and thymine behave very different from the other base vibrations. The carbonyl vibrations in 5′-rUMP and poly(rU) have broad band widths in the order of 35 cm^{-1}. The band width is 30 cm^{-1} in 3′-dTMP. The Gaussian component in the band shapes indicates a strong coupling between the carbonyl mode and the hydrogen atom of water modes through hydrogen bonds. In double-stranded structures, the band shape is less Gaussian and the band widths of the carbonyl modes are smaller. This is probably the result of a smaller distribution of hydrogen-bond distances and angles due to the restrictions imposed on the base–base hydrogen bonds by the secondary structure.

The vibrational dynamics of the band at 1575 cm^{-1} in adenine is partially determined by vibrational dephasing by water molecules and further depends on the nucleotide conformation. The band width is broader in single-stranded structures and mononucleotides as compared to double-stranded structures. This corresponds to the lifetime of the hydrogen bonds in base pairing, approximately 1 ms, which can be regarded as static on the Raman time scale.

The studies of the Raman band widths of synthetic polynucleotides revealed a dynamic picture on a (sub)picosecond time scale. Different base vibrations are sensitive to different dynamical degrees of freedom in the system. We have argued that backbone dynamics, hydrogen bonding, as well as solvent accessibility influences the vibrational band widths.

This work is supported by the Netherlands Organization for the Advancement of Research (NWO).

REFERENCES

1. Oxtoby, D. W. & Rice, S. A. (1976) *Chem. Phys. Lett.* **42,** 1–7.
2. Schweizer, K. S. & Chandler, D. (1982) *J. Chem. Phys.* **76,** 2296–2314.
3. Rothschild, W. G. (1984) *Dynamics of Molecular Liquids,* John Wiley & Sons, New York.
4. Diestler, D. J. (1976) *Chem. Phys. Lett.* **39,** 39–44.
5. Fisher, S. F. & Laubereau, A. (1975) *Chem. Phys. Lett.* **35,** 6–12.
6. Metiu, H., Oxtoby, D. W. & Freed, K. F. (1977) *Phys. Rev. A* **15,** 361–371.
7. Oxtoby, D. W. (1979) *J. Chem. Phys.* **70,** 2605–2610.
8. Lynden-Bell, R. M. (1977) *Mol. Phys.* **33,** 907–921.
9. Morresi, A., Mariani, L., Distefano, M. R. & Gior-

gini, M. G. (1995) *J. Raman Spectrosc.* **26,** 179–216.
10. Schroeder, J., Schiemann, V. H., Sharko, P. T. & Jonas, J. (1977) *J. Chem. Phys.* **66,** 3215–3226.
11. Rothschild, W. G. (1976) *J. Chem. Phys.* **65,** 455–462.
12. Kato, T. & Takenaka, T. (1979) *Chem. Phys. Lett.* **62,** 77–81.
13. Forester, T. R. & McDonald, I. R. (1991) *Mol. Phys.* **72,** 643–660.
14. Gillen, K. T. & Griffiths, J. E. (1972) *Chem. Phys. Lett.* **17,** 359–364.
15. Bartoli, F. J. & Litovitz, T. A. (1972) *J. Chem. Phys.* **56,** 404–412.
16. Finney, J. L., Goodfellow, J. M. & Poole, P. L. (1982) in *Structural Molecular Biology, Methods and Applications*, Davies, D. B., Saenger, W. & Danyluk, S. S., Eds., Plenum Press, New York.
17. Ohmine, I. & Tanaka, H. (1993) *Chem. Rev.* **93,** 2545–2566.
18. Brahms, S., Fritsch, V., Brahms, J. G. & Westhof, E. (1992) *J. Mol. Biol.* **223,** 455–461.
19. Letellier, R., Ghomi, M. & Taillandier, E. (1987) *J. Biomol. Struct. Dynam.* **4,** 663–683.
20. McGammon, J. A. & Karplus, M. (1983) *Acc. Chem. Res.* **16,** 187–193.
21. Montrose, C. J., Bucaro, J. A., Marshall-Coakley, J. & Litovitz, T. A. (1974) *J. Chem. Phys.* **60,** 5025–5029.
22. Terpstra, P. A., Otto, C. & Greve, J. (1993) *Biophys. Chem.* **48,** 113–122.
23. de Mul, F. F. M. & Greve, J. (1993) *J. Raman Spectrosc.* **24,** 245–250.
24. Gilson, T. R. & Hendra, P. J. (1970) *Laser Raman Spectroscopy*, John Wiley & Sons, Ltd., London.
25. Toyama, A., Takino, Y., Takeuchi, H. & Harada, I. (1993) *J. Am. Chem. Soc.* **115,** 11092–11098.
26. Toyama, A., Hanada, N., Abe, Y., Takeuchi, H. & Harada, I. (1994) *J. Raman Spectrosc.* **25,** 623–630.
27. Terpstra, P. A., Otto, C., Segers-Nolten, G. M. J., Kanger, J. S. & Greve, J. (1995) *Biospectroscopy* **1,** 255–263.
28. Nafie, L. A. and Peticolas, W. L. (1972) *J. Chem. Phys.* **57,** 3145–3155.
29. Clark, J. H. R. (1980) in *Advances in Infrared and Raman Spectroscopy*, Vol. 4, Clark, J. H. R. & Hester, R. E., Eds., Heyden & Sons, Ltd., London.
30. Hill, N. E. (1954) *Proc. Phys. Soc.* **67B,** 149–158.
31. Vincent-Geisse, J., Soussen-Jacob, J., Breuillard, C., Briquet, J. C. & Nguyen-Tan, T. (1977) *Mol. Phys.* **43,** 145–159.
32. Navarro, R., Hernanz, A. & Bratu, I. (1994) *J. Chem. Soc. Faraday Trans.* **90,** 2325–2330.
33. Maroncelli, M. (1991) *J. Chem. Phys.* **94,** 2084–2103.
34. Maroncelli, M. & Fleming, G. R. (1988) *J. Chem. Phys.* **89,** 5044–5069.
35. Rosenthal, S. J., Xie, X., Du, M., & Fleming, G. R. (1991) *J. Chem. Phys.* **95,** 4715–4718.
36. van Woerkom, P. C. M., de Bleyser, J., de Zwart, M. & Leyte, J. C. (1974) *Chem. Phys.* **4,** 236–248.
37. Saenger, W. (1984) *Principles of Nucleic Acid Structure*, Springer-Verlag, New York.
38. Majoube, M. (1985) *Biopolymers* **24,** 2357–2369.
39. Fasman, G. D., Ed. (1975) *Handbook of Biochemistry and Molecular Biology*, 3rd ed., CRC Press, Cleveland, OH.
40. Fisher, S. F. & Laubereau, A. (1978) *Chem. Phys. Lett.* **55,** 189–196.
41. Robertson, G. N. & Yarwood, J. (1978) *Chem. Phys.* **32,** 267–282.
42. Walrafen, G. E., Fisher, M. R., Hokmabadi, M. S. & Yang, W. H. (1986) *J. Chem. Phys.* **85,** 6970–6982.
43. Terpstra, P., Combes, D. & Zwick, A. (1990) *J. Chem. Phys.* **92,** 65–70.
44. Nuutero, S., Fujimoto, B. S., Flynn, P. F., Reid, B. R., Ribeiro, N. S. & Schurr, J. M. (1994) *Biopolymers* **34,** 463–480.
45. Bevington, P. R. (1969) *Data Reduction and Error Analysis for Physical Sciences*, McGraw-Hill, New York.